Electronic Supplementary Material (ESI) for Catalysis Science & Technology.

Supporting Information

Synergistic effect on BCN nanomaterials for the oxygen reduction reaction– A kinetic and mechanistic analysis to explore the active sites

E.A. Anook Nazer and Azhagumuthu Muthukrishnan*

*School of Chemistry, Indian Institute of Science Education and Research Thiruvananthapuram, Maruthamala (P.O), Vithura-695551, Kerala, India

Email: muthukrishnan@iisertvm.ac.in

Materials

Graphite powder (>99) and sodium nitrate (99.99%) were purchased from Sigma Aldrich. Sulphuric acid (98%), potassium permanganate (98.5%), hydrogen peroxide (30%), hydrochloric acid (37%) and boric acid (99.99%) were obtained from Merck. Dicyandiamide (>98%) was obtained from TCI.

Powder X-ray Diffraction spectroscopy

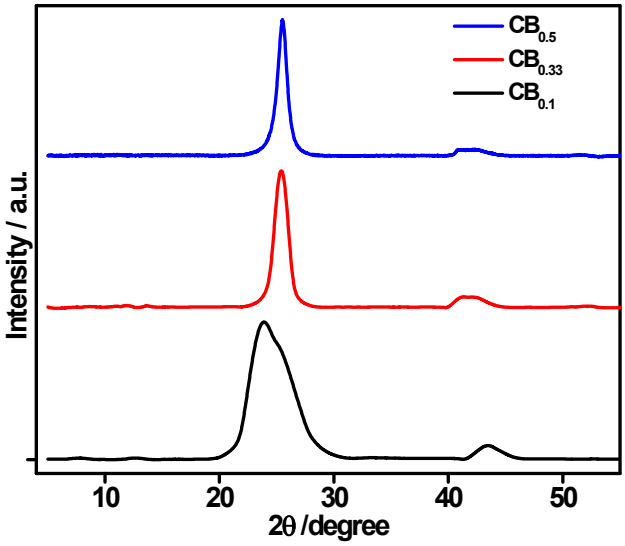

Figure S1. PXRD pattern of B-rGO compounds at various initial boron content.

Chracterization

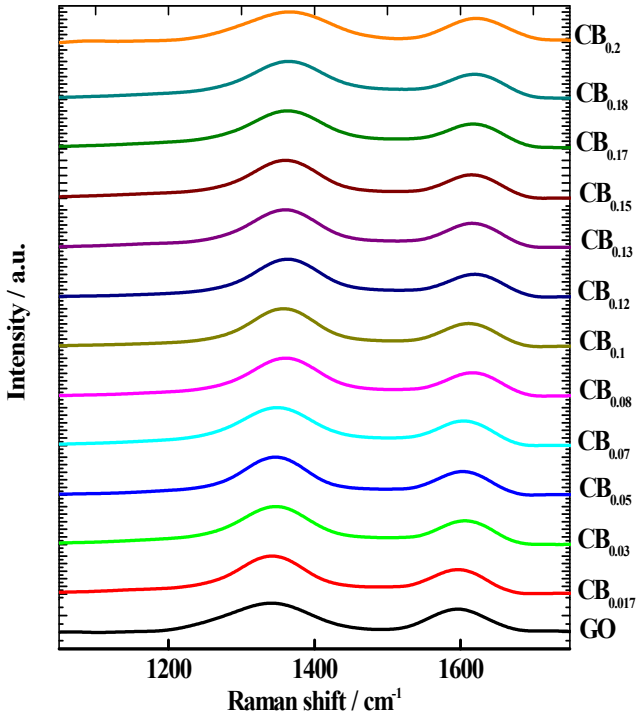

Figure S2. Raman spectra of B-rGO compounds at the various initial boron contents compared with the GO.

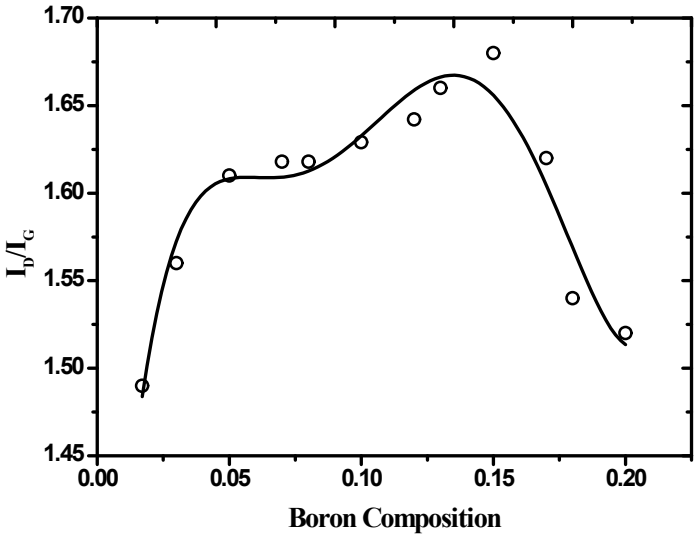

Figure S3. Initial boron content (numbers in the x-axis indicate the fraction of the boron reference to the carbon, example C : B = 1:*n*, where *n* represents the values in the x-axis).solid line indicates the polynomial fitting (5^{th} order) of the values.

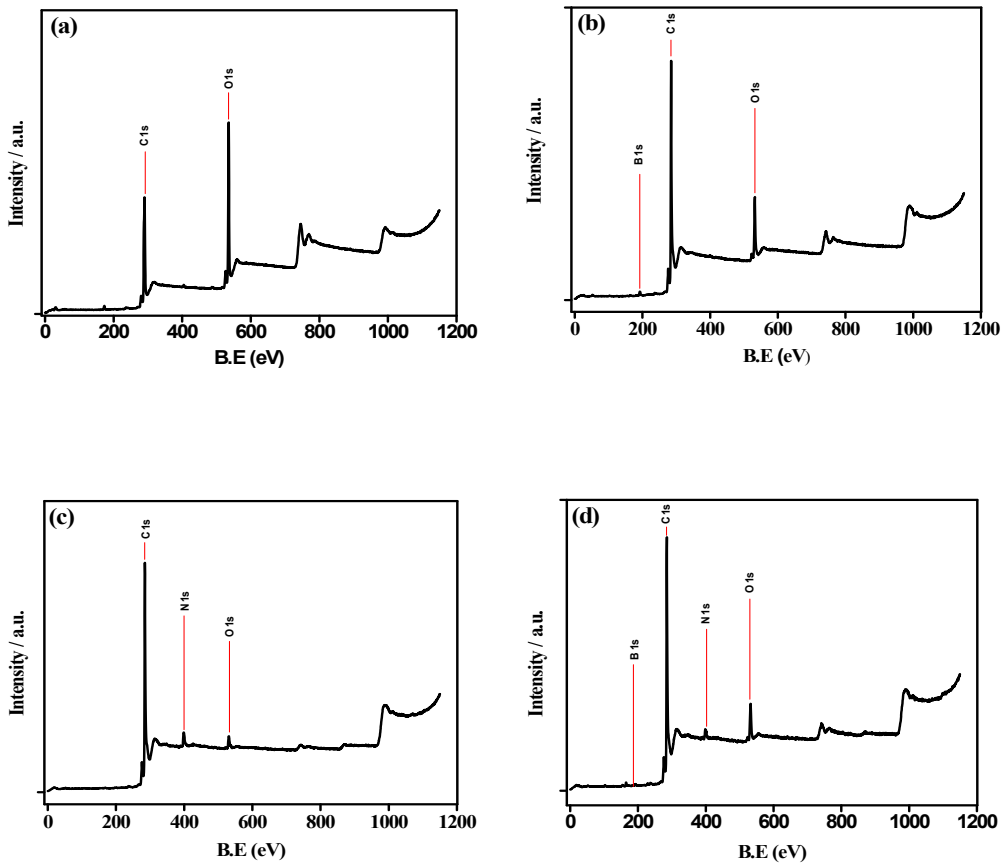

Figure S4. XPS survey spectra of the compounds (a) GO, (b) B-rGO, (c) N-rGO and (d) B&N-rGO.

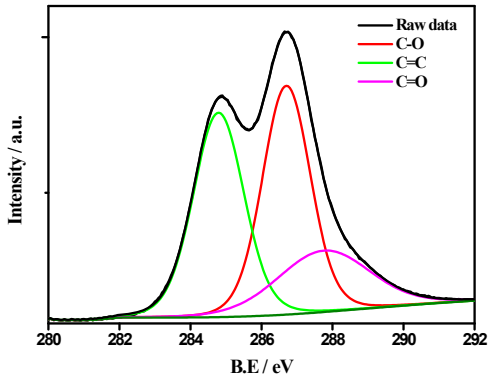

Figure S5. Core level C-1s XPS spectrum of GO, deconvoluting into various oxygen functionalities.

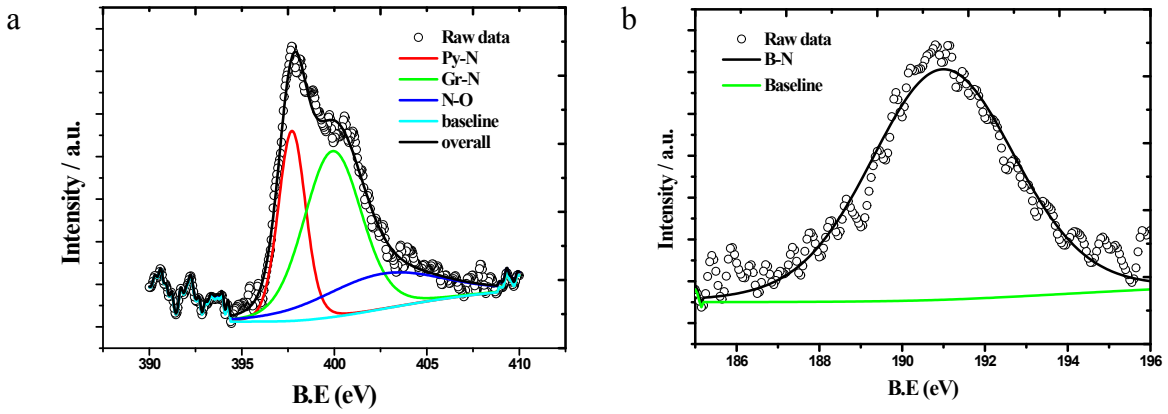

Figure S6. Core level (a) N-1s and (b) B-1s XPS spectra of the B-rGO+N-rGO

The existence of the B and N is observed in the physical mixture of 1:1 ratio B-RGO and N-RGO compounds. The shift in the N-1s spectra to the low binding energy side is observed due to the interaction with the electropositive element (Boron) demonstrated the existence of the B-N interaction. In the physical mixture, the Py-N and Gr-N peaks are appeared at 397.7 eV and 399.9 eV, respectively. This is 0.3 to 0.4 eV shift from the values observed for B&N-RGO and N-RGO. Besides, the B-1s spectra shifts to the higher binding energy (191.0 eV) compared with the B&N-RGO (189.4 eV), indicating the interaction of boron with the higher electronegative element, i.e. nitrogen. The formation of chemical

bonds between B and N could shift the peak to the larger extent. Rao et al. [Panchakarla, Adv. Mater., 2009, **21**, 4726-4730] reported the formation of the B-N bonds during the copyrolysis of activated charcoal with boric acid and urea. The deconvoluted N-1s peak at 397.1 eV corresponds to B-N bond, which is approximately 1 eV shift from the normal C-N (pyridinic nitrogen) bond. Hence the physical mixture of B-rGO and N-rGO does not have any chemical bonds. Also, the B-rGO and N-rGO were synthesised separately, the B and N present in two different layers of graphene. Hence, The B-rGO and N-rGO may interact due to their electronegativity difference in the uniformly dispersed solution.

a

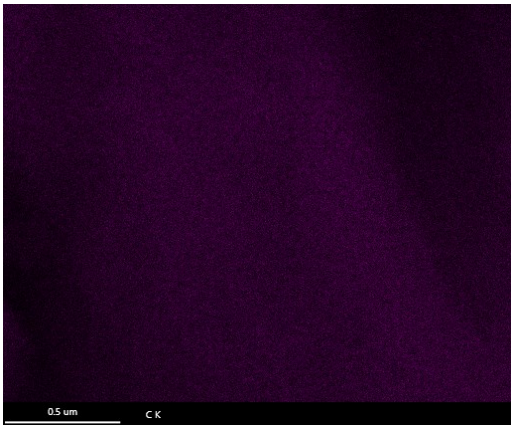

b

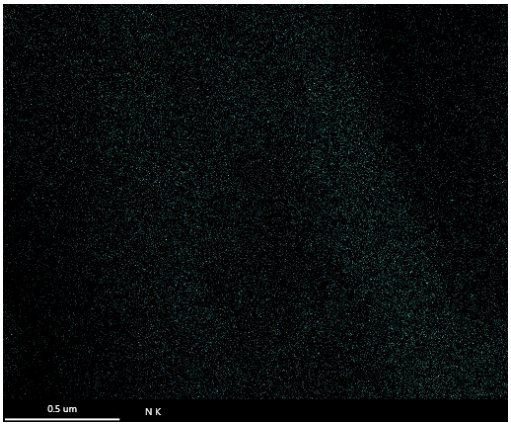

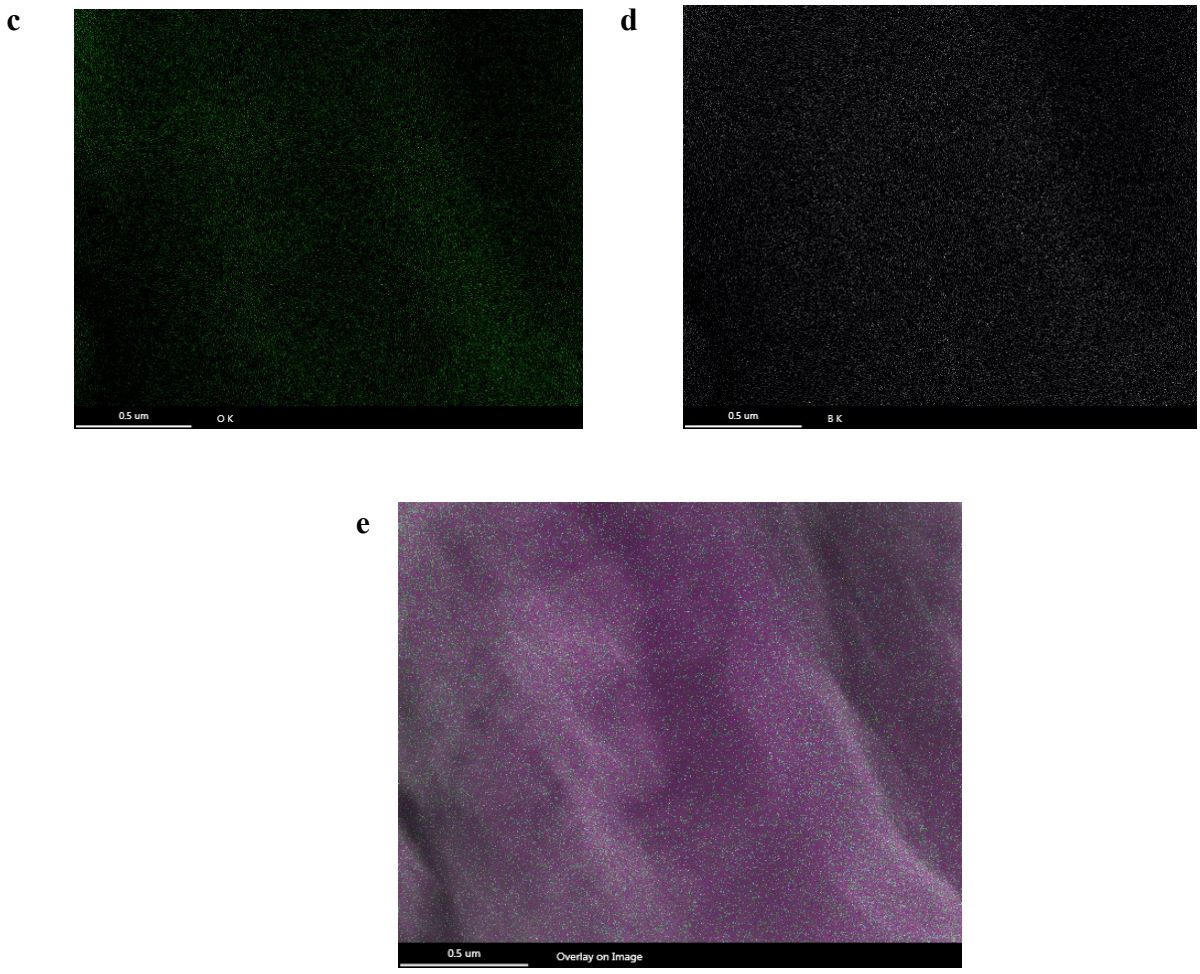

Figure S7. Elemental mapping of individual atoms present in the B&N-rGO are shown for the elements C (a), N (b), O (c), B (d) and overlap of all the above (e).

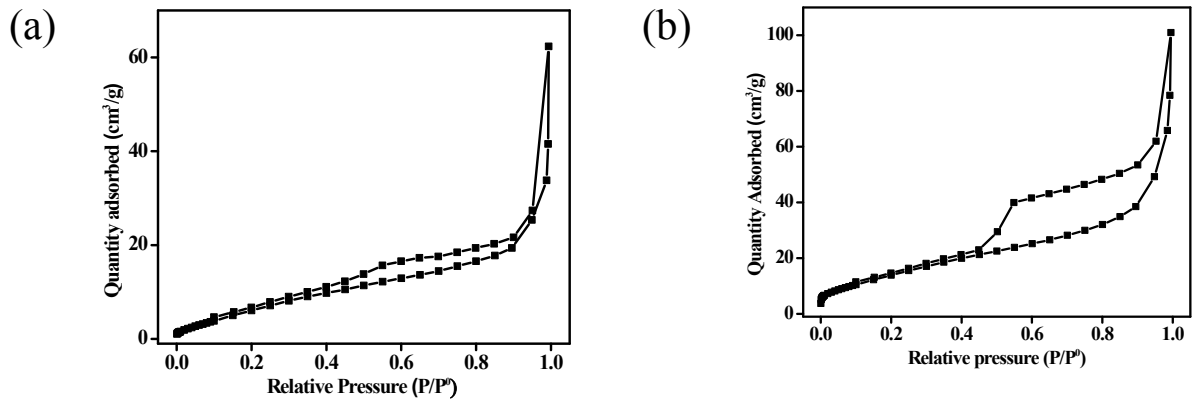

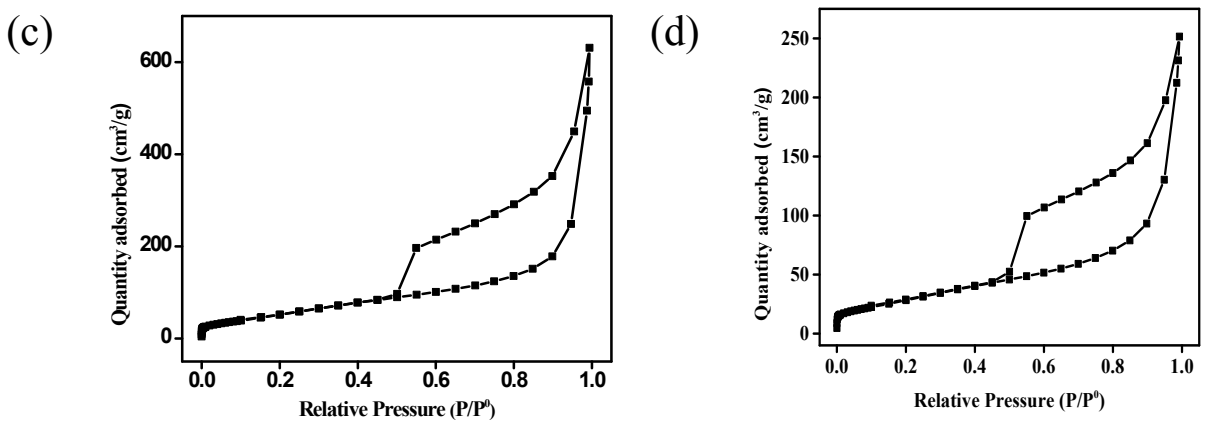

Figure S8. BET isotherms of (a) GO, (b) B-rGO, (c) N-rGO and (d) B&N-rGO

Electrochemistry

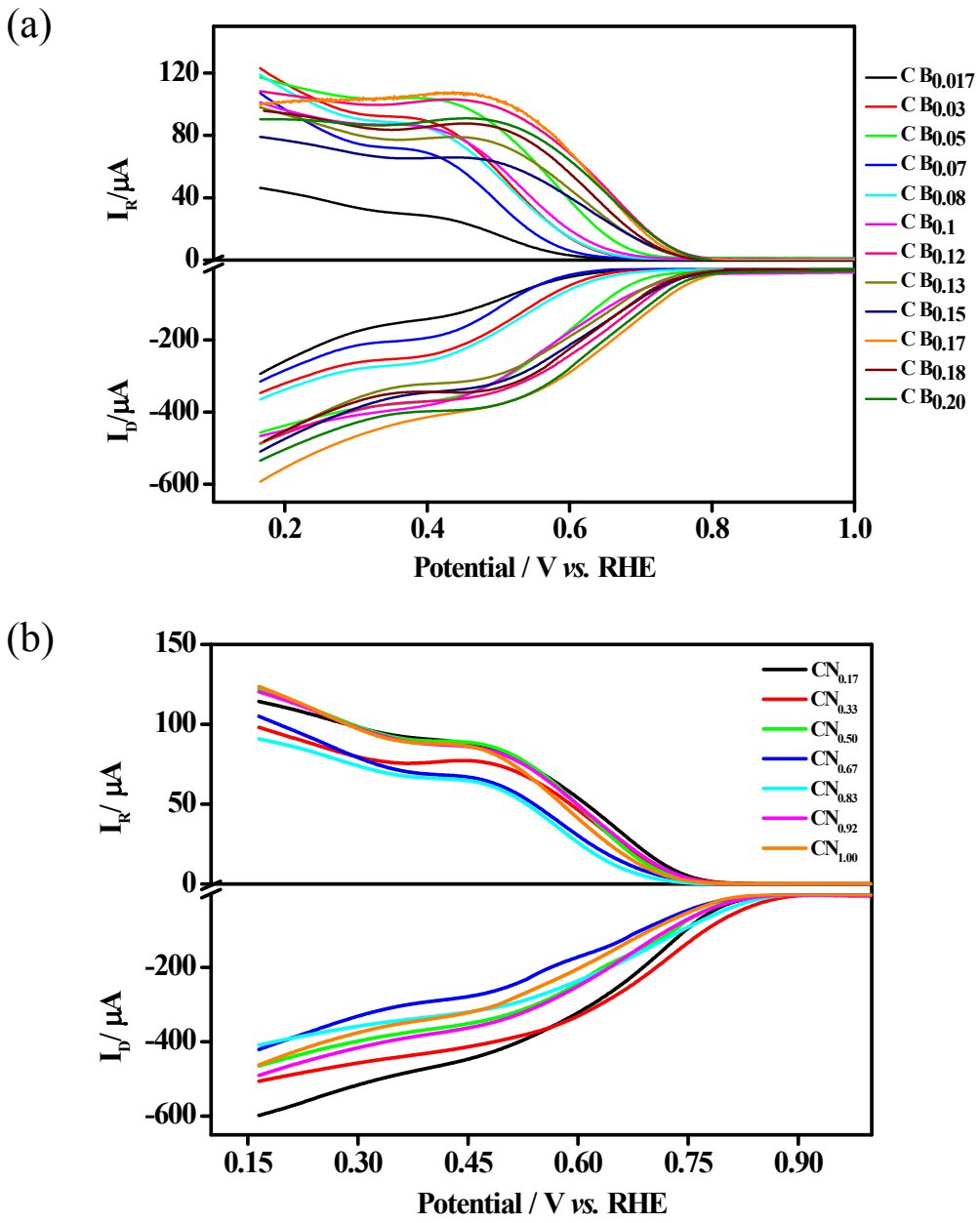

Figure S9. RRDE voltammograms for the ORR on (a) B-rGO and (b) N-rGO at various amounts of initial boron and nitrogen precursor at O_2-saturated 0.1 M KOH.

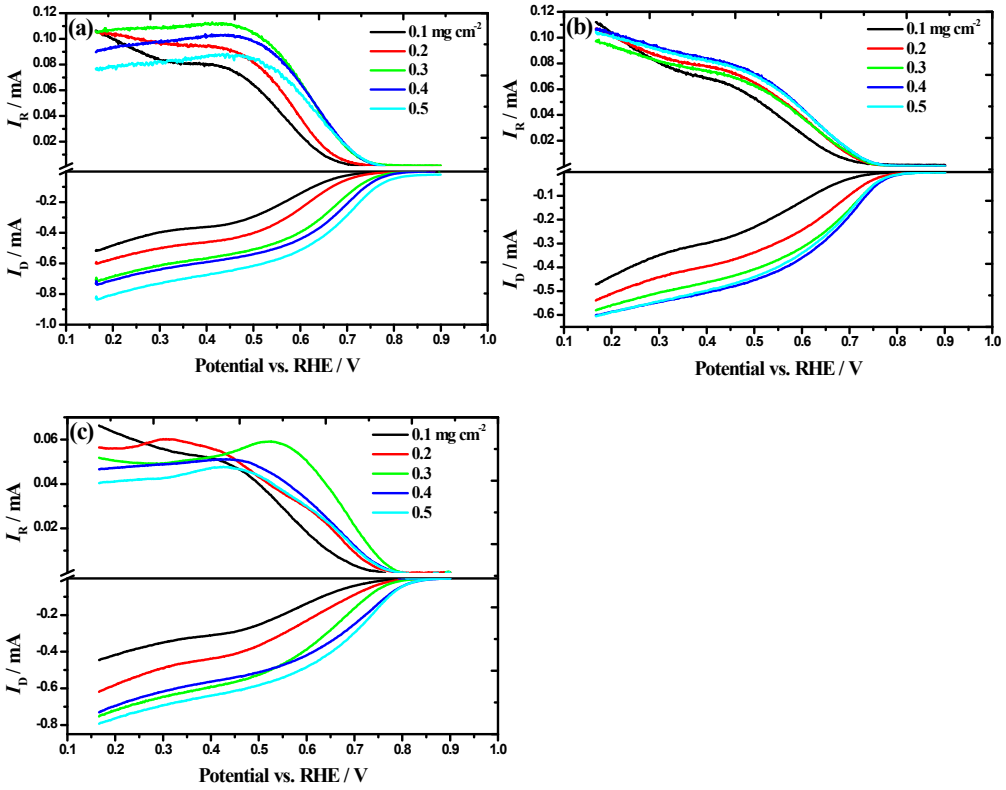

Figure S10. RRDE voltammograms of the ORR on (a) B-rGO, (b) N-rGO and (c) B&N-rGO catalysts at various loading densities. The rotation speed is 1600 rpm, and at the scan rate of 10 mV/sec.

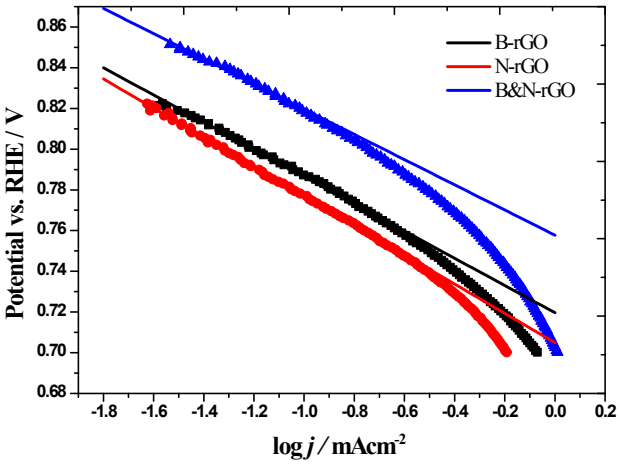

Figure S11. Tafel plots of the ORR on B-rGO, N-rGO and B&N-rGO. The Current densities are taken in the kinetic-controlled region, i.e. close to the onset potential.

Table S1: BET Surface area measurement for all the three catalysts.

Compound	BET S.A (m^2 g^{-1})	Pore size (nm)	Pore Volume (cm^3 g^{-1})
GO	25.8	15.0	0.10
B-rGO	51.3	12.3	0.16
N-rGO	187.1	21.1	0.99
B&N-rGO	100.5	15.6	0.39

Table S2: The onset potentials of all the three compounds studied.

Loading density (mg cm^{-2})	Onset potential vs. RHE (V)*		
	N-rGO	B-rGO	B&N-rGO
0.1	0.736	0.742	0.765
0.2	0.762	0.789	0.79
0.3	0.797	0.803	0.803
0.4	0.813	0.806	0.842
0.5	0.827	0.804	0.843

*the onset potential is the potential at which the current reaches 0.1 mA cm^{-2}.

Table S3: Tafel slopes for the compounds studied in this work

Compounds	Tafel slope (mV dec^{-1})
B-rGO	66.8
N-rGO	71.9
B&N-rGO	61.8

Damjanovic model

The kinetics of the ORR was studied using the Damjanovic model shown below

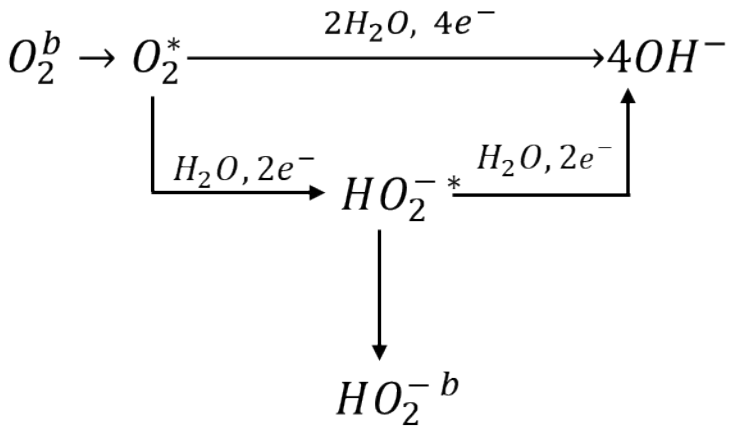

Scheme S1. Kinetic model for the ORR proposed by Damjanomic et al. *b* and * refers the bulk and surface concentrations, respectively. The direct pathway is the reduction of O_2 to H_2O by 4-electron. The stepwise reduction of O_2 to H_2O_2 by 2e (k_2) followed by the reduction of H_2O_2 to H_2O by 2e (k_3).

The number of electron (n) and the percentage of H_2O_2 estimated using the disk and ring currents from the rotating ring-disk electrode voltammetry. The equations are as shown below

$$n = \frac{4I_D}{I_D + \frac{I_R}{N}} \qquad \text{and} \qquad \%H_2O_2 = \frac{200\ \frac{I_R}{N}}{I_D + \frac{I_R}{N}}$$

From the mass balanced equations of the above kinetic model gives rise to the linear relations between I_D/I_R and $I_{DL}/(I_{DL}\text{-}I_D)$ and inverse square root of rotational speeds as shown below

$$\frac{I_D}{I_R} = \frac{1+\frac{2k_1}{k_2}}{N} + \frac{2\left(1+\frac{k_1}{k_2}\right)}{NZ_2} k_3 \omega^{\frac{-1}{2}} \quad \text{and} \quad \frac{I_{DL}}{I_{DL}-I_D} = 1 + \frac{k_1+k_2}{Z_1}\omega^{\frac{-1}{2}}$$

where, I_D – Disk current (A)

I_R – Ring current (A)

I_{DL} – Limiting current density (A)

N – Collection efficiency (0.37)

ω – Rotational speed (s^{-1})

$k_1, k_2 \; and \; k_3$ – Rate constants (as explained in the Scheme S1).

$Z_1 = 0.62 D_{O_2}^{2/3} v^{-1/6}$

$Z_2 = 0.62 D_{H_2O_2}^{2/3} v^{-1/6}$

D_{O_2} – Diffusion coefficient of O_2 at 0.1 M KOH (1.9×10^{-5} cm^2 s^{-1})

$D_{H_2O_2}$ – Diffusion coefficient of H_2O_2 at 0.1 M KOH (1.27×10^{-5} cm^2 s^{-1})

v – kinometic viscosity (0.01 cm^2 s^{-1})

The slopes and intercept of the plots $\frac{I_D}{I_R} vs. \omega^{\frac{-1}{2}}$ and $\frac{I_{DL}}{I_{DL}-I_D} vs. \omega^{\frac{-1}{2}}$ from the above equations are given below

$$I_1 = \frac{1+\frac{2k_1}{k_2}}{N}, \quad S_1 = \frac{2\left(1+\frac{k_1}{k_2}\right)}{NZ_2} k_3 \quad \text{and} \quad S_2 = \frac{k_1+k_2}{Z_1}$$

where, I_1 – intercept of $\frac{I_D}{I_R} vs. \omega^{\frac{-1}{2}}$ plot

S_1 – slope of $\frac{I_D}{I_R} vs. \omega^{\frac{-1}{2}}$ plot

S_2 – slope of $\frac{I_{DL}}{I_{DL} - I_D} vs. \omega^{\frac{-1}{2}}$ plot